Near-limit Detonation in Long Spiral Tube: Improved Design and Methodology

Zhaoyuan Huang, Zihang Ni, Zongtai Li, Zifeng Weng, and Rémy Mével
Center for Combustion Energy, School of Vehicle and Mobility, State Key Laboratory of Automotive Safety and Energy, Tsinghua University, Beijing, China

1 Introduction

While the Chapman-Jouguet (CJ) theory can predict with good accuracy the detonation velocity away from the detonability limits, it does not take into account the boundary conditions and associated losses, and cannot predict the near-limit detonation behavior [1]. As the detonability limit is approached, the detonation wave does not propagate steadily anymore and may demonstrate a variety of unstable behaviors. Lee et al. [2] monitored quasi-continuously the detonation front velocity using microwave Doppler interferometry and proposed six detonation propagation modes. The first mode is observed away from the limits and is characterized by a stable and steady propagation velocity. The velocity is close to the CJ speed (D_{CJ}). The second mode is characterized by low-amplitude and high-frequency oscillations of the detonation speed. A velocity deficit in the range 10-20% of D_{CJ} may be observed. These two regimes can be observed for both regular and irregular detonations. For highly irregular mixtures, the detonation may propagate according to different unstable modes, referred to as stuttering (third mode), and galloping (fourth mode). A stuttering detonation typically propagates at an average velocity around 0.7 D_{CJ} and its speed demonstrate both large-amplitude, low-frequency oscillation, and low-amplitude, high-frequency oscillations. A galloping detonation propagates at an average velocity in the range 0.5-0.7 D_{CJ} with very large-amplitude (0.5 to 1.5 D_{CJ}), low-frequency velocity fluctuations. The fifth mode corresponds to the low-velocity mode which propagates at 0.4-0.5 D_{CJ} with fluctuations of few m/s. Low-velocity detonations are composed of a reaction zone and a leading shock wave separated by a large distance [3]. Beyond this regime, detonation failure (mode 6) is taking place. Unstable detonation modes are favored by small diameter tube, low-pressure conditions, and high irregularity of the mixture. Near-limit detonations have been studied for 70 years [4–6] and many studies have employed long straight tube/channel to observe the repetitive cycles of detonation failure and re-initiation that characterize unstable detonation regimes. Few years ago, Jackson et al. [7] proposed a new design to study unstable detonation. This approach relies on the utilization of a long, transparent tube, coiled as a spiral (4 mm inner diameter and 30 m in length), and enables observing the detonation propagation over a very long time using a single high-speed camera operating at 12,000 frame per second (fps). Only a stoichiometric propane-oxygen mixture was employed and the initial pressure was in the range P_0=7-20 kPa. Cao et al. [8, 9] employed a similar approach but monitored the wave propagation using 83 photodiodes. They employed CH_4, C_2H_2, and C_3H_8 mixed with O_2 or N_2O, and possibly diluted with up to 70% Ar. Several tubes with lengths in the range 8.2-32.8 m and inner diameters of 3.2-25.4 mm were used, and P_0 was varied in the range 2.5-42 kPa.

The goals of the present study were to: (i) develop an improved design for the spiral detonation tube facility; (ii) propose an improved post-processing procedure to extract the velocity of unstable detonation; (iii) introduce the wavelet transform approach to characterize the regimes of detonation propagation.

Correspondence to: mevel@mail.tsinghua.edu.cn

2 Materials and Methods

2.1 Spiral tube design and experimental characteristics

Figure 1 shows the experimental setup, including (a) gas preparation section, (b) spiral tube, (c) ignition system, (d) trigger and imaging system. The test section in Fig. 1(b) consists of a circular tube made of transparent polyurethane and two acrylic square sheets. The actual test section is presented in Fig. 1(e). A spiral channel with a diameter of 6 mm was carved in one acrylic sheet. The tube was installed in the channel and was covered with the other acrylic sheet. The inner and outer diameters of the tube are 4 mm and 6 mm, respectively. The smallest and largest diameters of the spiral are 68.25 mm and 360.75 mm, which corresponds to 32.5 cycles and a total length of 43.8 m. The spiral tube of the present apparatus is 46% longer than the one in [7]. In each experiment, the spiral tube is vacuumed to below 100 Pa, and then filled with combustible mixture prepared in section (a) using the partial pressure method. A glow plug is activated remotely to ignite the mixture. The flame transits from deflagration to detonation when propagating through the Shchelkin spiral located in (c). The detonation wave then enters the test section via the outer part of the spiral. A light sensor is used to trigger the high-speed camera which operated at 25,000 fps with a resolution of 896×896 px^2. Compared to the settings in [7], our frame rate is 108% higher, while the error is 15% lower, based on the error analysis method proposed by Jackson et al. [7]. With the above improvements on the experiment setup, we are able to record the near-limit detonation behaviour for a longer time and with higher resolution and accuracy.

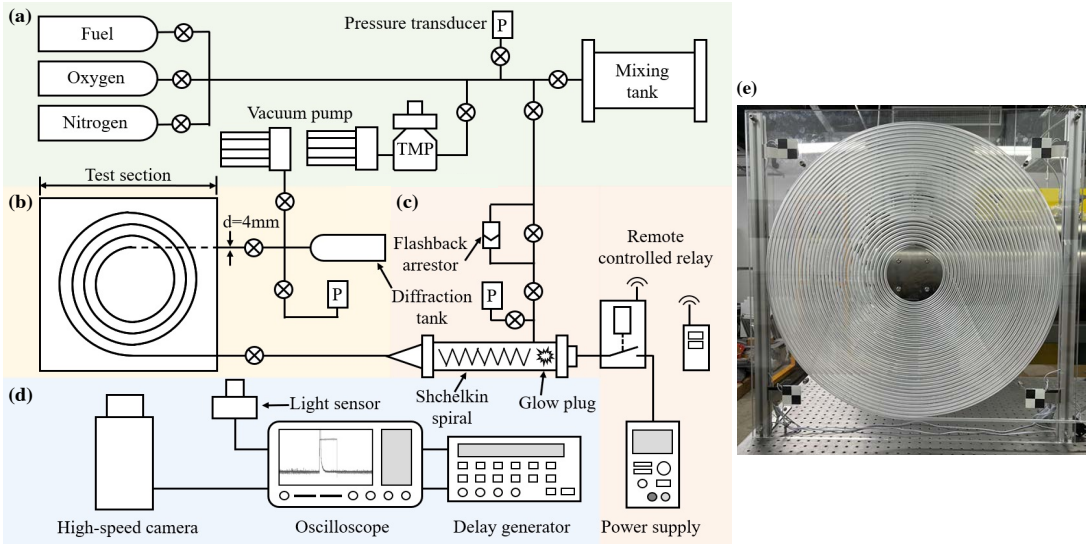

Figure 1: Experimental setup for near-limit detonation study in long spiral tube. (a) Gas preparation section, (b) spiral tube, (c) ignition system, (d) trigger and imaging system, (e) actual setup.

2.2 Image Processing

The imaging system provides chemiluminescence images of detonation propagating in the spiral tube. These images were processed following the flow chart given in Fig. 2. In the first step, possible geometric distortions are corrected, considering that the camera cannot be perfectly perpendicular to the test section. Four reference black-and-white squares with backward illumination were installed at the four corners of the test section, as shown in Fig. 1(e). The centers of these squares were located at the corner of a 0.6×0.6 m^2 square and were accurately determined in each frame using OpenCV library.

The geometric distortion of the image can be captured by the corresponding distortion of the square and can thus be corrected accordingly. The second step of image processing is to detect the detonation front. Since the luminous signal detected occupies several pixel in the radial direction, uncertainty exists in the determination of detonation front position. In Fig. 3(a), we show that the semi-width of the luminous band occupies four pixels which corresponds to about 3.3 mm. This issue has been noted in [7] and results in fluctuations in the radial direction of the detonation front position. To avoid such an issue, we first find the forefront pixel that can be detected in the circumferential direction, i.e., the pixel with the largest θ; then the pixel is projected onto the spiral function we used to design the spiral channel, i.e., $r = 363 - 9\theta/2\pi$ (with r in mm). These operations are illustrated in Fig. 3(b). In the third step, the positions of the detonation front determined in two successive frames were used to calculate the detonation velocity using forward difference.

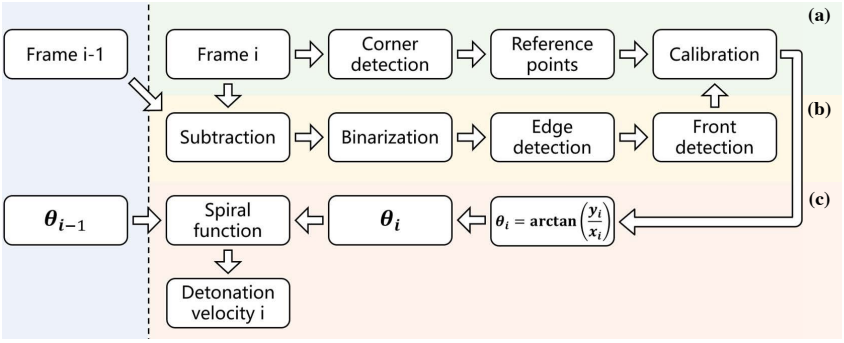

Figure 2: Flow chart of the present image processing. (a) Geometric distortion correction, (b) detonation front detection, (c) detonation speed calculation.

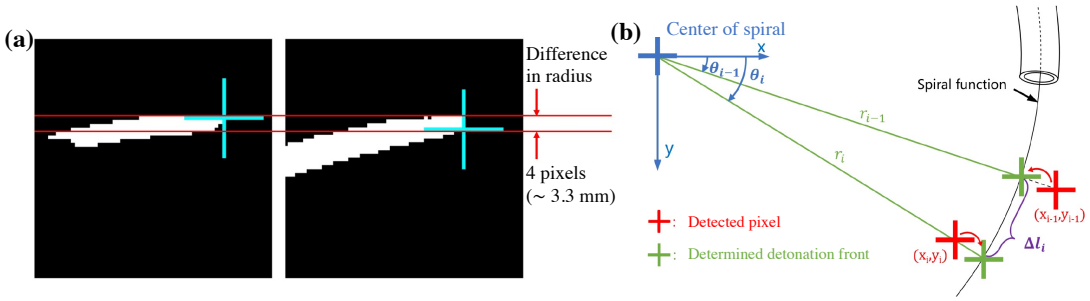

Figure 3: Image processing for the determination of the detonation front position. (a) Uncertainty of detonation front in radial direction; (b) Correction of detonation front in spiral coordinate.

2.3 Wavelet Analysis

In previous works, spectral analysis has been found useful to characterize the dynamic behavior of near-limit detonation. For example, Jackson et al. [7] used fast Fourier transform (FFT) to determine the dominant frequency of detonation speed variation. However, these frequencies might change with time, which cannot be captured by FFT. To overcome such a limitation, we applied the wavelet transform approach. Continuous wavelet transform (CWT) is widely used to study time-series data [10]. Unlike Fourier analysis, both time and frequency resolution can be obtained by CWT. This makes it possible to use CWT to characterize the time-resolved dynamic behavior of near-limit detonation. A CWT numerical method was introduced by Grinsted et al. [10] using the Morlet wavelet. A wavelet is a function

with zero mean and localized in both frequency and time [10]. We employed the popular Morlet wavelet function, which is defined as [11]:

$$\Psi_0(\eta) = \pi^{-\frac{1}{4}} e^{i\omega_0\eta} e^{-\frac{\eta^2}{2}} \tag{1}$$

where η is a non-dimensional time parameter, i is the imaginary unit, and ω_0 is the dimensionless frequency. Wavelet function can be translated and dilated/contracted to generate a series of daughter wavelets. For the discrete data series, the wavelet transform takes the form [11]

$$W_n(s) = \sum_{n'=1}^{N} \left(\frac{\delta\tau}{s}\right)^{1/2} f(t)\Psi^*_{s,t}\left(\frac{(n'-n)\delta\tau}{s}\right), \tag{2}$$

where n is the discrete time index; $\Psi^*_{s,t}(t)$ is the complex conjugate of the daughter wavelet; s is the scale dilation parameter; N is the number of data points in the time series; and $\delta\tau$ is the time difference between two consecutive data points. The basic idea behind the CWT is that each daughter wavelet corresponds to a band-pass filter in the Fourier domain with given central frequency and width [10]. Thus applying wavelet transform to the velocity time-series enables to determine the local frequencies of the detonation fron speed fluctuations as a function of time.

3 Results and Discussion

Two series of experiments were performed with propane-oxygen mixtures; both mix 1 and 2 have an equivalence ratio Φ=1. The initial pressure was varied in the range 3.5-20 kPa. Figure 4 (a) shows the evolution of the average detonation velocity ($\bar{D}$) as a function of $P_0^{-1}d^{-1}$, where d is the tube diameter. It demonstrates the reasonable agreement obtained between our data and the data from the literature when using the scaling law proposed by Jackson et al. [7]. Figure 4 (b) shows the evolution of the average detonation velocity as a function of P_0. It indicates that the data can be divided into three regions: (i) in the high-velocity regime, from 14.1 to 20 kPa, $\bar{D}$ is above 0.9 D_{CJ} and varies little with P_0; (ii) in the intermediate-velocity regime, in the range 10.3-14 kPa, a high sensitivity to P_0 is observed with $\bar{D}$ varying from 0.9 D_{CJ} to below 0.65 D_{CJ}; (iii) in the low-velocity regime, P_0 less than 10.3 kPa, the sensitivity of $\bar{D}$ to P_0 is weak with variations in the range 0.55-0.65 D_{CJ}.

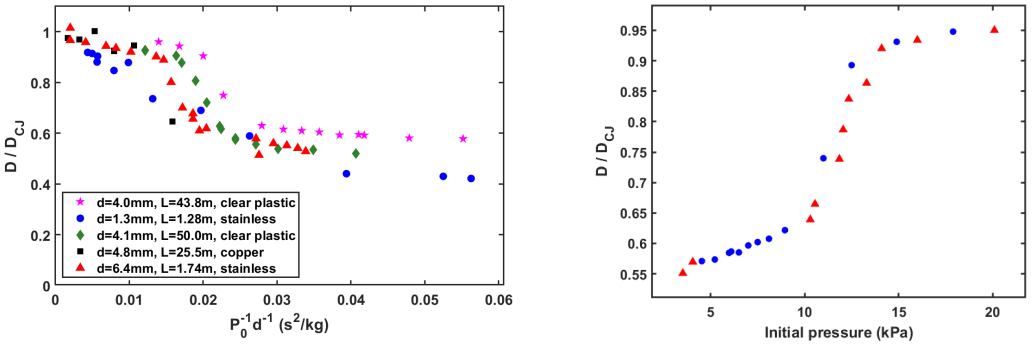

(a) Comparison with previous results (b) Present results for both mix 1 and 2

Figure 4: Evolution of the average detonation velocity as a function of (a) $P_0^{-1}d^{-1}$, and (b) P_0. In (a): pink stars are for mix 1 and the other symbols are from [7]. In (b): blue dots are for mix 1, and red triangles are for mix 2. In all cases, stoichiometric propane-oxygen mixtures were used.

Figure 5 shows the detonation propagation in the (a) high- and (b) intermediate-velocity regimes. In the high-velocity regime, the detonation is characterized by a bright and elongated reaction zone, followed by a long and less luminous trailing feature. No obvious difference were observed between the

successive frames in terms of chemiluminescence signal. In the intermediate-velocity regime, successive failure and re-initiation of the detonation are observed. For failed detonation, the reaction zone is much less bright and elongated, and the trailing feature disappears. During re-initiation, a very bright spot appears for few frames, and the characteristics observed in the high-velocity regime are rapidly re-established until the next failure takes place. In the low-velocity regime, detonations demonstrate similar features as in the intermediate-velocity regime with successive failure and re-initiation events, but occurring more frequently.

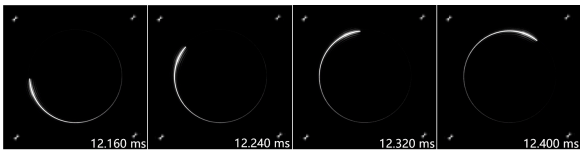

(a) High-velocity regime, P_0=17.9 kPa

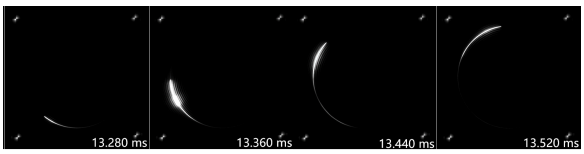

(b) Intermediate-velocity regime, P_0=11.8 kPa

Figure 5: Direct imaging of detonation chemiluminescence in the high- (stable propagation) and intermediate-velocity (stuttering propagation) regimes. In both cases, mix 1 was used.

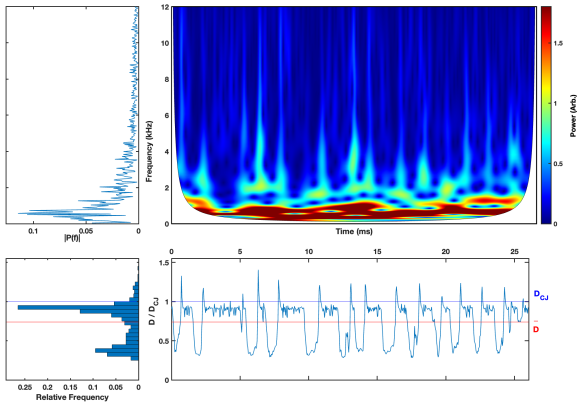

(a) Intermediate-velocity regime
Stuttering, P_0=11.9 kPa

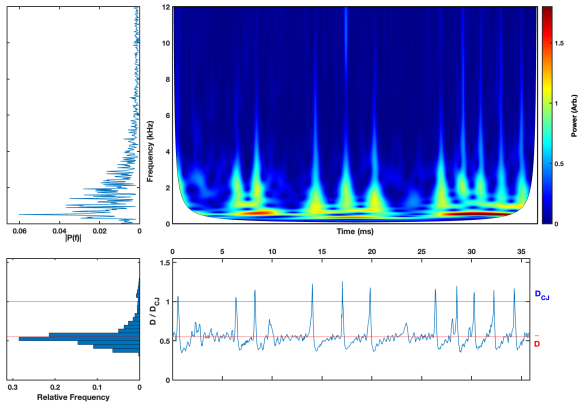

(b) Low-velocity regime
Galloping, P_0=3.5 kPa

Figure 6: Evolution of the instantaneous velocity of the detonation front and corresponding wavelet and Fourier transforms, as well as velocity distribution. In both cases, mix 2 was used.

Further insight can be gained by analyzing the evolution of the instantaneous velocity of the detonation front, as shown in Figure 6 for the intermediate- (stuttering) and low-velocity regimes (galloping).
In the high-velocity regime (not shown), only rapid and weak oscillations of the detonation front velocity are observed. The distribution of speed is narrow with a mean velocity just below D_{CJ}. The wavelet power spectrum is characterized by a quasi-single color, which indicates a wide range of existing frequencies with similar power. In addition, weak elongated vertical features are also present and are representative of fast transients. All these features are characteristics of a stable detonation.
In the intermediate-velocity regime, shown in Figure 6 (a), the front velocity demonstrates much larger variations. The detonation can propagate for several ms at a velocity close to D_{CJ} and exhibits rapid velocity fluctuations. The velocity profile also demonstrates much larger oscillations and reach velocities as low as 0.4 D_{CJ}. Such detonation failure events are followed by very rapid increases of the velocity up to 1.4 D_{CJ}, which correspond to detonation re-initiation. The velocity distribution is much broader and characterized by a two modes with one velocity peak just below D_{CJ} and another peak centered around 0.4 D_{CJ}. The mean velocity is around 0.8 D_{CJ}. The wavelet power spectrum is characterized by a

quasi-continuous band of high power located at a low frequency around 800-1000 Hz. The most violent re-initiation events results in elongated vertical features with power significantly above the background level. In addition, velocity fluctuations with frequencies above 4000 Hz are observed as the detonation propagates at a velocity close to D_{CJ}. All these features are characteristics of a stuttering detonation.
In the low-velocity regime, shown in Figure 6 (b), the detonation front velocity oscillates between 0.4 and 1.2 D_{CJ}. Rapid and relatively low-amplitude oscillations are observed as the detonation propagates at a low velocity. Re-initiation events are also taking place and are characterized by a very rapid acceleration of the detonation front, almost immediately followed by a strong deceleration, as the detonation front cannot sustain at all stable propagation at high velocity. The time interval between re-initiation events is rather irregular, and failed re-initiation events can be clearly identified in the velocity profile. The distribution of velocity is rather narrow and demonstrates a single mode with a peak centered around 0.5 D_{CJ}, which is also close to the average velocity. The wavelet power spectrum exhibits localized bands of high power at frequencies in the range 500-1000 Hz. However, these regions are disconnected from each other, as failed re-initiation events are taking place. In between successful re-initiation events, the dominant frequencies are in the range 2000-2500 Hz. Successful re-initiation events result in sharp elongated vertical features with wide base of triangular shape. All these features are characteristics of a galloping detonation.

4 Conclusion

We have developed a long spiral tube facility to investigate the behavior of near-limit detonation in a stoichiometric propane-oxygen mixture. The highly compact design and the faster high-speed camera that we employed enabled to significantly increase the amount of data obtained as compared to previous studies. As the initial pressure was decreased, we successively observed stable, stuttering, and galloping detonation propagation. The use of wavelet transform allowed us to visualize the change of intrinsic frequency of the detonation front velocity during the highly unstable propagation in the stuttering and galloping regimes. Future work will focus on further characterizing the dynamics of stuttering and galloping detonation by quantitatively studying the repetitive cycle of detonation failure and re-initiation.

References

[1] Lee JHS (2008. The Detonation Phenomenon. Cambridge University Press.

[2] Lee JJ, Dupré G, Knystautas R, Lee JH (1995). Shock Waves 5(3):175

[3] Manzhalei VI (1999). Combustion, Explosion and Shock Waves 35(3):296.

[4] Mooradian AJ, Gordon WE (1951). Journal of Chemical Physics 19(9):1166.

[5] Edwards DH, Morgan JM (1977). Journal of Physics D: Applied Physics 10(17):2377.

[6] Haloua F, Brouillette M, Lienhart V, Dupré G (2000). Combustion and flame 122(4):422.

[7] Jackson S, Lee BJ, Shepherd JE (2016). Combustion and Flame 167:24

[8] Cao W, Gao, D, Ng HD, Lee JHS (2019). Proceedings of the Combustion Institute 37(3):3555.

[9] Cao W, Ng HD, Lee JHS (2020). Shock Waves 30(7):713.

[10] Grinsted A, Moore JC, Jevrejeva S(2004). Nonlinear processes in geophysics 11(5/6):561

[11] Torrence C, Compo GP (1998). Bulletin of the American Meteorological society 79(1):61